

Supplementary Information for:

Ball milling as an effective route for the preparation of doped bornite: synthesis, stability and thermoelectric properties

G. Guélou, A. V. Powell and P. Vaqueiro*

Department of Chemistry, University of Reading, Whiteknights, RG6 6AD

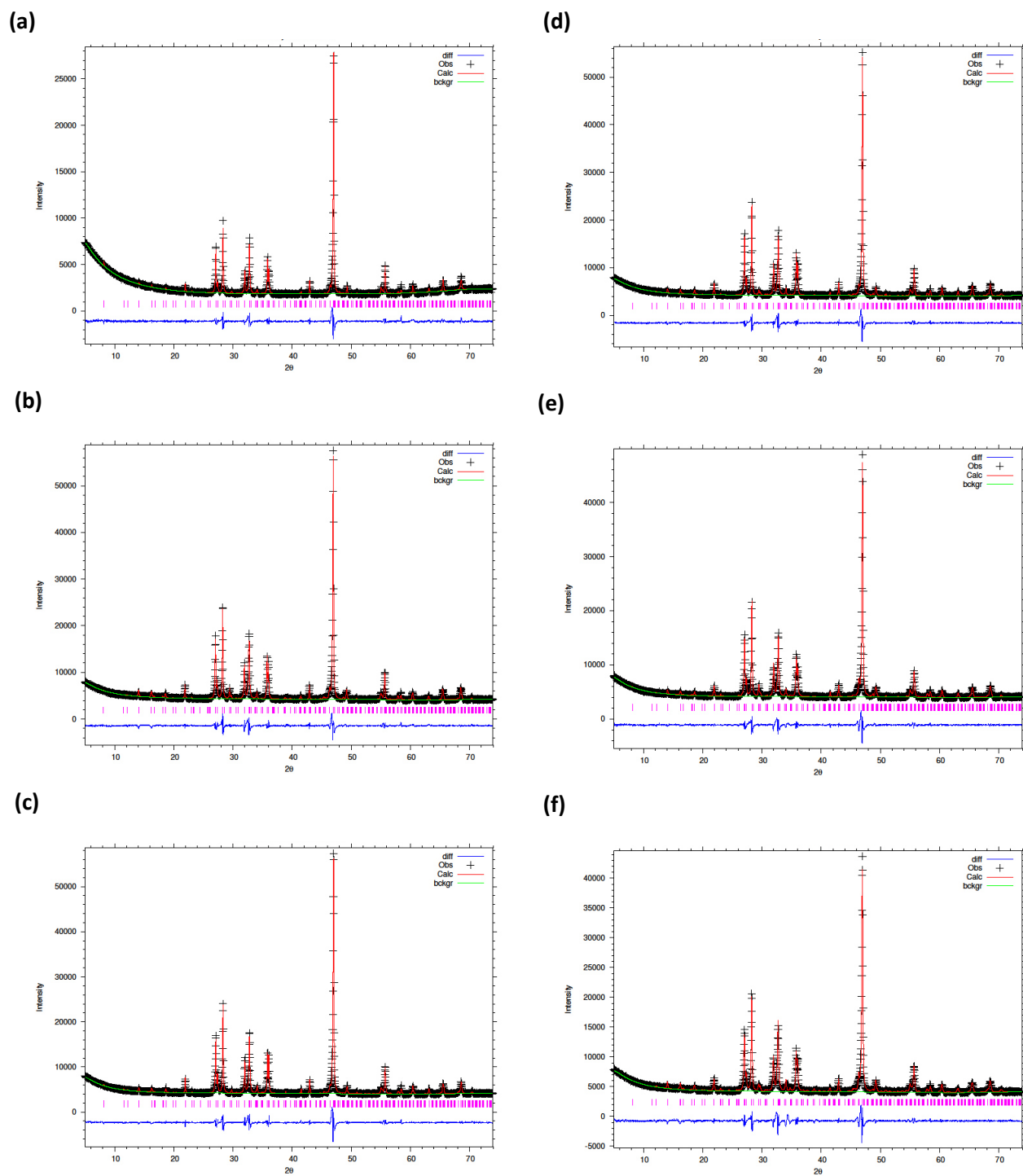
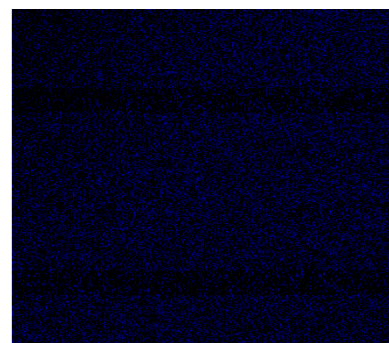
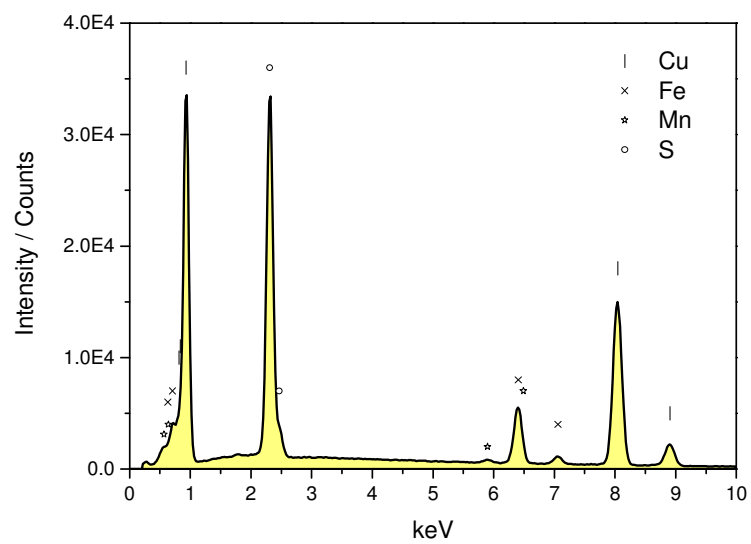
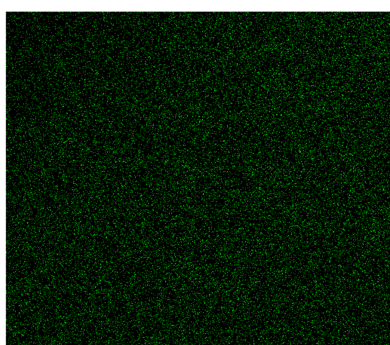


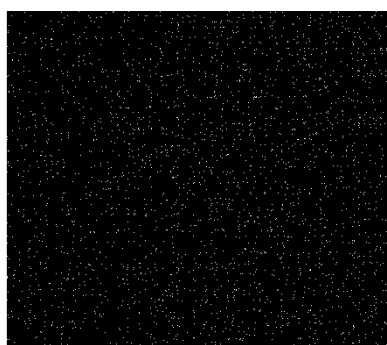
Fig. S1 Le Bail refinement using X-ray diffraction data of the consolidated $\text{Cu}_5\text{Fe}_{1-x}\text{Mn}_x\text{S}_4$ pellets, (a) $x = 0.01$ ($R_{\text{wp}} = 4.21\%$), (b) $x = 0.02$ ($R_{\text{wp}} = 3.97\%$), (c) $x = 0.03$ ($R_{\text{wp}} = 4.29\%$), (d) $x = 0.04$ ($R_{\text{wp}} = 3.96\%$), (e) $x = 0.05$ ($R_{\text{wp}} = 3.77\%$) and (f) $x = 0.10$ ($R_{\text{wp}} = 4.15\%$). Observed (black crosses), calculated (red line) and difference (lower blue line) profiles are plotted. Reflection positions for the orthorhombic phase (top) are marked.



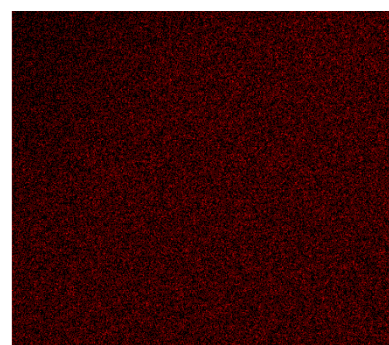
Cu Ka1



Fe Ka1



Mn Ka1



S Ka1

Fig. S2 EDX spectrum and elemental maps for a consolidated sample of $\text{Cu}_5\text{Fe}_{0.95}\text{Mn}_{0.05}\text{S}_4$.

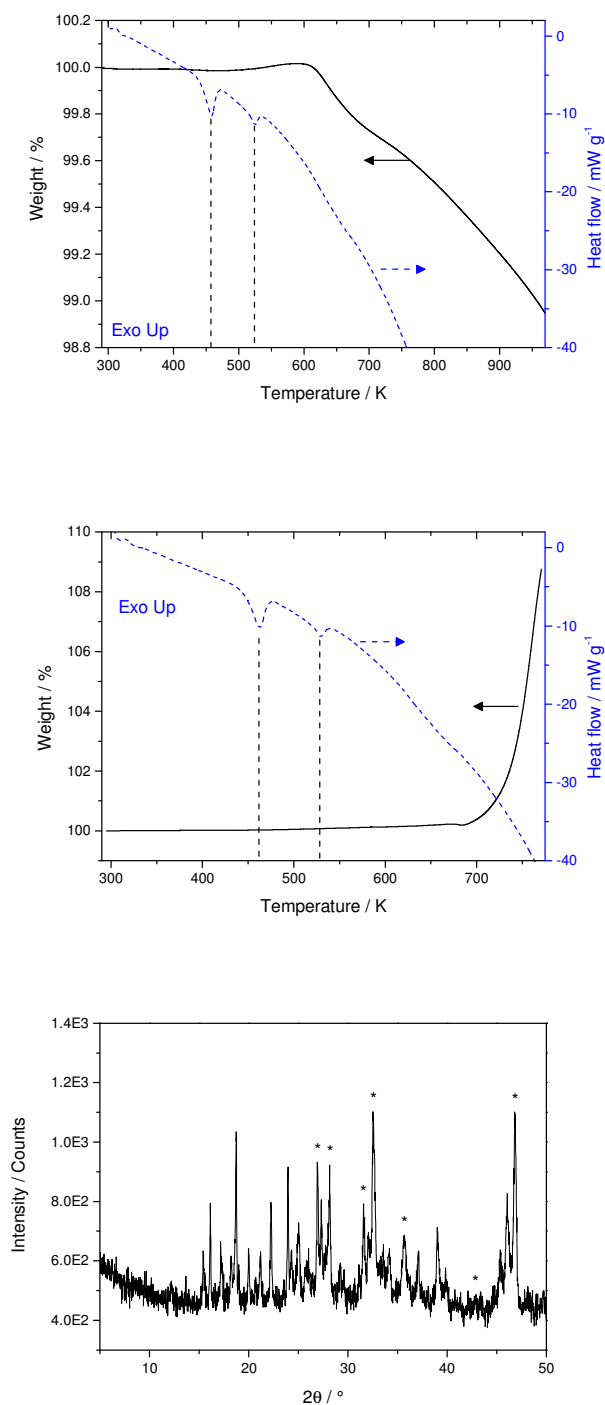


Fig. S3 Combined TGA/DSC data for Cu_5FeS_4 powder under nitrogen flow (top) and in air (middle), showing the temperature dependence of the weight percentage of the sample (solid black line) and the heat flow (dashed blue line). Graph at the bottom shows the powder X-ray diffraction pattern for bornite after the TGA/DSC in air, with peaks corresponding to bornite marked. Remaining peaks correspond to a mixture of copper sulfate oxides and copper sulfide.

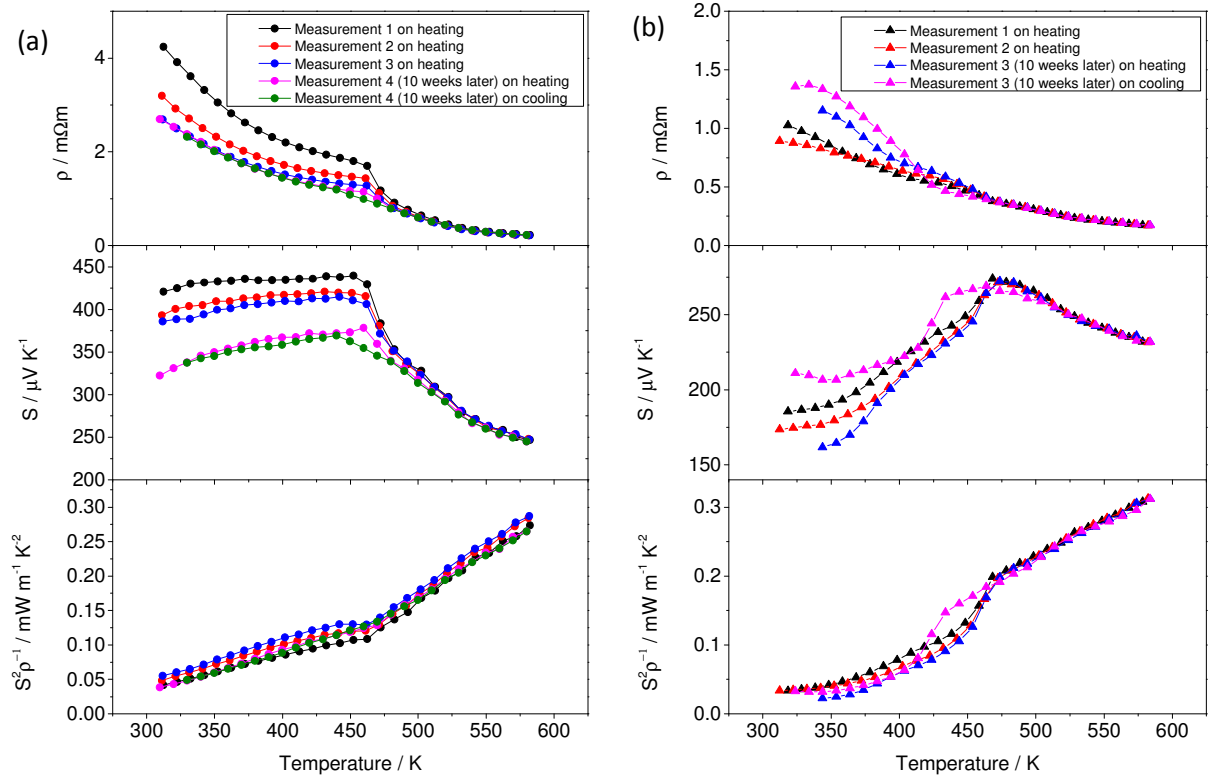


Fig. S4 Repeated measurements on heating and cooling of the electrical resistivity (top), the Seebeck coefficient (middle) and the resulting power factor (bottom) as a function of temperature for (a) Cu_5FeS_4 and (b) $\text{Cu}_5\text{Fe}_{0.96}\text{Mn}_{0.04}\text{S}_4$.

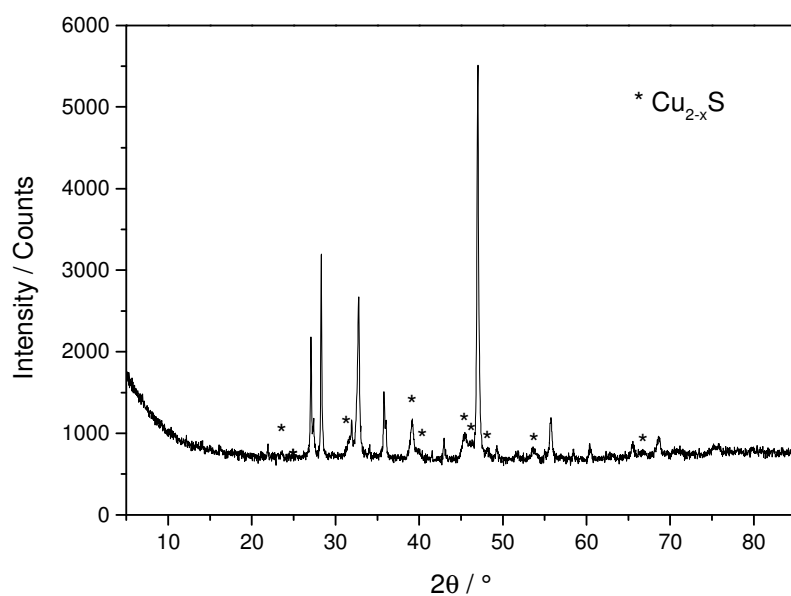


Fig. S5 Powder X-ray diffraction data of Cu_5FeS_4 after measurements of electrical transport property up to 890 K. The impurity peaks corresponding to Cu_{2-x}S are marked.

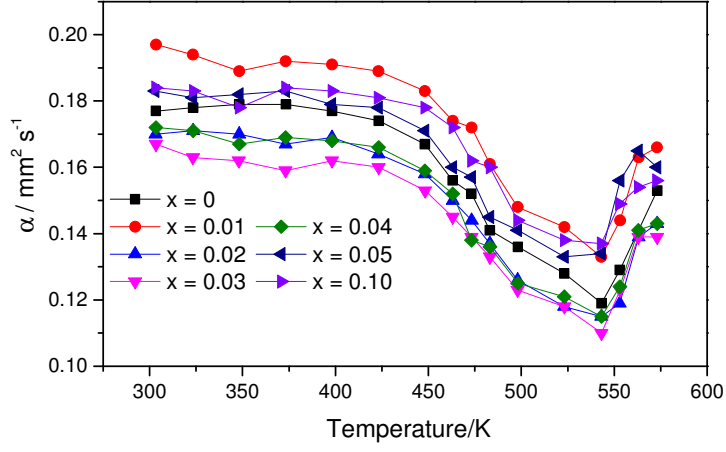


Fig. S6 Temperature dependence of the thermal diffusivity, α , of $\text{Cu}_5\text{Fe}_{1-x}\text{Mn}_x\text{S}_4$.

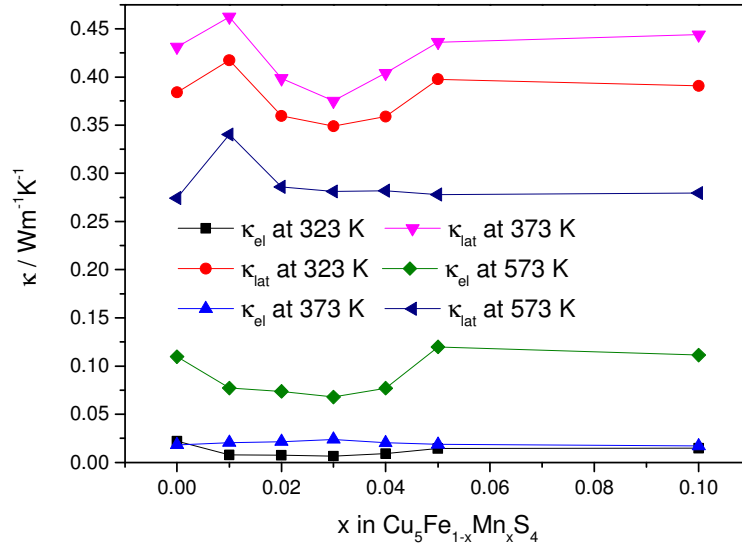


Fig. S7 Estimated lattice and electronic components of the thermal conductivity of $\text{Cu}_5\text{Fe}_{1-x}\text{Mn}_x\text{S}_4$ as a function of x , calculated using Wiedemann-Franz law, with $L = 2.44 \times 10^{-8} \text{ W } \Omega \text{ K}^{-2}$.